Articles

Syntheses and Optical Properties of the Water-Dispersible ZnS:Mn Nanocrystals Surface Capped by L-Aminoacid Ligands: Arginine, Cysteine, Histidine, and Methionine

Ju Ho Lee,† Yong Ah Kim, Kimoon Kim, Young Duk Huh, June Won Hyun,‡ H. S. Kim,‡ S. J. Noh,† and Cheong-Soo Hwang*

*Department of Chemistry and †Department of Applied Physics, Dankook University, Institute of Nanosensor and Biotechnology, Seoul 140-714, Korea. *E-mail: cshwang@dankook.ac.kr*

Received May 1, 2007

Water dispersible ZnS:Mn nanocrystals were synthesized by capping the surface of the nanocrystals with four kinds of aminoacids ligands: arginine, cystein, histidine, and methionine. The aminoacids capped ZnS:Mn nanocrystal powders were characterized by XRD, HR-TEM, EDXS, and FT-IR spectroscopy. The optical properties of the aminoacids capped ZnS:Mn colloidal nanocrystals were also measured by UV/Vis and solution photoluminescence (PL) spectroscopies in aqueous solvents. The solution PL spectra showed broad emission peaks around 575 nm (orange light emissions) with PL efficiencies in the range of 4.4 to 7.1%. The measured particle sizes for the aminoacid capped ZnS:Mn nanocrystals by HR-TEM images were in the range of 5.3 to 11.7 nm.

Key Words : ZnS:Mn nanocrystal, Aminoacid capping, Water soluble nanocrystal, Orange emitting nanophosphor

Introduction

Low-dimensional semiconductor nanocrystals have gained significant interest during the past decade.[1-4] These materials have been widely applied for non-linear optics or electronic devices and more recently in some advanced biotechnology area due to their unique physical, chemical and optical properties.[5-7] Among the most important characteristics for those nanosized semiconductors their optical properties can be varied accordingly the size of the nanocrystals because the corresponding band gap energies are different even for the materials with the exactly identical elemental compositions.[8,9] Further, some modifications for the surface of the nanocrystals were made to increase their quantum efficiency as well as thermal stability. For instance, surface capped CdS and ZnS nanocrystals by strongly coordinating organic solvents produced monodisperse and highly luminescent nanoparticles.[10]

An orange light emitting manganese ion doped nanocrystallite, ZnS:Mn, is of special interest due to its high photoluminescence efficiency and stability at ambient temperature, which are critical properties required to be applied for commercial electro-luminescence devices.[11] Considerable progress has been also made in the preparation methods for those naonocrystal materials including gas, solid, and aqueous solution reactions *via* organometallic precursor routes. However, these methods often require high temperatures, pressures and even use of bio-hazard substances.[12]

Water dispersible semiconductor nanocrystals were developed for fluorescent labeling technologies especially to be applied in biomedical area.[13] Unfortunately, most highly luminescent semiconductor nanocrystals are grown in hydrophobic media so that they are hardly compatible with biological systems. There are several reports of solubilized hydrophobic nanocrystals in water.[14-16] According to those papers, the most commonly used synthetic scheme for the water dispersible nanocrystal is to use polar surface capping ligands such as mercaptoacetate (MAA) and sulfodiisooctyl succinate (AOT) molecules to form a micelle structure where the negative charges are distributed on the surface. In addition, it was shown that the photoluminescence efficiency for the AOT capped ZnS:Mn nanocrystal increased up several times after the surface modification.[14] This phenomenon resulted from the additional energy transfer of surfactant to Mn^{2+} metal ion as well as reducing the energy loss due to non-radioactive transition by the surface modification.

Amino acid ligands such as histidine[17] and cystein[18] have been developed as surface capping agents for undoped ZnS nanocrystals. They were found to be very effective capping ligands in the synthesis of narrow range size distributed nanocrystals, which is difficult to achieve in aqueous solution due to different dissociation constants for ZnS and MnS in water. A brief description of the synthesis of histidine coordinated ZnS:Mn nanocrystal has been appeared once in a literature.[19] However, thorough physical and

optical characterizations such as IR, XRD, EDXS, and PL efficiency calculations have not been reported for the material afterward. Early in our group, the synthesis and optical characterization of the water dispersible L-valine capped ZnS:Mn nanocrystal and the crystal structure of the precursor $[Zn(Val)_2(H_2O)]$ complex have been reported, which showed that an aminoacid ligand can be a promising biocompatible capping agent for the semiconductor nanocrystals.[20] In this paper, we now report the syntheses of the ZnS:Mn nanocrystals capped by four different aminoacids, which are commercially available, inexpensive and non biohazard materials, in mild reaction conditions. In addition, characterizations for their optical and physical properties as water-dispersible orange light emitting nanophosphors are described.

Experimental

All the solvents except deionized water were purchased from Aldrich (reagent grade) and distilled prior to use. The starting materials including L-arginine, L-cystein, L-histidine, L-methionine, $ZnSO_4$, $MnSO_4$, and Na_2S were purchased from Aldrich and used as received. The UV/Vis absorption spectrum was recorded on a Perkin Elmer Lamda 25 spectrophotometer equipped with a deuterium/tungsten lamp. The FT-IR spectrum was recorded on a Perkin Elmer spectrophotometer equipped an attenuated total reflection (ATR) unit. The solution photoluminescence spectra were taken by a Perkin Elmer LS-45 spectrophotometer equipped with a 500 W Xenon lamp, 0.275 m triple grating monochrometer, and PHV 400 photomultiplier tube. HR-TEM images were taken with a JEOL JEM 1210 electron microscope with a MAG mode of 1000 to 800000, and the accelerating voltage was 40-120 kV. The samples for the TEM were prepared *via* dispersion into methanol solvent and placement on a carbon-coated copper grid (300 Mesh) followed by drying under vacuum. In addition, the elemental compositions of the nanocrystals were determined by EDXS (Energy Dispersive X-ray Spectroscopy) spectra which were obtained *via* an EDXS collecting unit equipped in the HR-TEM, with a Si (Li) detector in IXRF 500 system.

Synthesis of aminoacids capped ZnS:Mn nanocrystals. Preparation procedures are slightly modified from the methods to prepare undoped ZnS nanocrystal capped by histidine[16] and cysteine[17] *via* formation of zinc (II)-aminoacid coordinated complexes as reactive intermediates in aqueous solution. A solution of $ZnSO_4 \cdot 5H_2O$ (1.44 g, 5 mmol) in 50 mL of water was slowly added to a 50 mL aqueous mixture solution containing 10 mmols of aminoacids and NaOH (0.40 g, 10 mmol) at 5 °C (ice-water bath). The solution was warmed up to ambient temperature after 1 hour stirring. Each resulting white powder was redissolved in a 50 mL of warm (*ca.* 60 °C) 1 M Tris buffer (Aldrich) solution. In another flask, $MnSO_4 \cdot H_2O$ (0.02 g, 0.1 mmol) and Na_2S (0.40 g, 5 mmol) was dissolved in a 20 mL of 0.01 M HCl solution. Then the mixture was transferred to the flask containing Zn-aminoacid complexes under vigorous stirring. The resulting solution refluxed for 20 hours. Slow cooling to ambient temperature and an addition of ethanol solution resulted in yellow-white precipitations at the bottom of the flask. Finally, the obtained solids were separated *via* centrifuge and decanting the supernatant. Then the solids were dried for 24 hours in a vacuum oven. The obtained experimental data are summarized in Table 1.

The PL efficiencies for the aminoacid capped ZnS:Mn nanocrstals were measured and calculated by following the same method reported by Williams *et al.*[21] which is to calculate a relative quantum yield by comparing to a standard material in literature.[22] 0.1 M solution of quinine sulfate in H_2SO_4 (Fluka) in our case, whose emission wave length and reported absolute quantum yield are 550 nm and 0.546 (at 22 °C) respectively. The used excitation wavelength for the standard (quinine sulfate) was obtained from the UV/Vis spectrum for each aminoacid capped ZnS:Mn nanocrystal. The emission spectra for both standard and aminoacid capped ZnS:Mn nanocrystal were recorded at five different concentrations in aqueous solvents. Then we plotted a graph of integrated fluorescence intensity versus absorbance for both samples obtained at different concentrations. As a result we were able to obtained straight lines with fairly constant gradients, and their intercepts were at zero. Finally, the relative PL efficiencies were calculated by using the following equation[21]:

Table 1. Experimental data summary for the aminoacids capped ZnS:Mn nanocrystals

	ZnS:Mn (Arg)	ZnS:Mn (Cys)	ZnS:Mn (His)	ZnS:Mn (Met)
UV/Vis (λ_{max}, nm)	322	296	316	317
PL emission wavelength (nm)	575	573	575	576
PL efficiency (%)	5.2	6.5	4.4	7.1
FT-IR ν (cm^{-1})	3332 (m), 3181 (m), 2954 (m), 2878 (m), 1655 (m), 1635 (m), 1451 (m), 1406 (m), 1350 (m), 1116 (s), 998 (m)	3387 (m), 3018 (m), 2969 (m), 2917 (m), 2747 (m), 2672 (m), 2585 (m), 2084 (m), 1619 (m), 1583 (m), 1486 (m), 1406 (s), 1383 (m), 1338 (m), 1297 (m), 1194 (m), 1124 (m), 1090 (m), 963 (m), 874 (m), 847 (m), 778 (m)	3127 (m), 3007 (m), 2620 (m), 1592 (m), 1504 (m), 1404 (m), 1343 (m), 1269 (m), 1118 (s), 1011 (m), 964 (m), 926 (m), 820 (m), 776 (m)	3211 (m), 2923 (m), 1619 (m), 1387 (m), 1338 (m), 1140 (s), 997 (m), 962 (m), 884 (m), 775 (m)
HR-TEM image (average particle size, nm)	6.7	11.7	5.3	8.3

$$\Phi_x = \Phi_{ST}\left(\frac{Grad_x}{Grad_{ST}}\right)\left(\frac{\eta_x^2}{\eta_{ST}^2}\right)$$

In this equation, Φ represents PL efficiency. The subscript ST and *x* denote the standard (quinine sulfate) and the aminoacids capped ZnS:Mn nanocrystal respectively. In addition, 'Grad' indicates the gradient from the plot of integrated fluorescence intensity versus absorbance, and 'η' represents the refractive index of the solvent which we could eliminate this factor by using the same solvent for both standard and the nanocrystal.

Results and Discussion

Figure 1 shows UV/Vis absorption spectra of the corresponding aminoacids capped ZnS:Mn nanocrystal. In most cases, broad absorption peaks appeared from 296 to 322 nm and the maxima are located around 300 nm in average. The values are quite close to that of the valine capped ZnS:Mn nanocrystal, 305 nm.[20] Figure 2 presents the solution PL spectra obtained from the corresponding aminoacids capped ZnS:Mn in aqueous solution, in which broad emission peaks appeared around 575 nm wavelengths. The corresponding emission spectra were obtained when the excitation wave lengths were fixed at corresponding UV/Vis absorption peaks; 322 nm (Arg), 296 nm (Cys), 316 nm (His), and 317 nm (Met) respectively. The excitation spectra were also obtained when the corresponding emission wave lengths were fixed at 575 nm (Arg), 573 nm (Cys), 575 nm (His), and 576 nm (Met) respectively. The observed large Stoke shifts for the amonoacids capped ZnS:Mn nanocrystals are among the typical features appeared in nano-sized crystalline materials. For instance, a similar feature has been observed for the water soluble AOT capped CdS nanocrystal. The excitation peak appeared at 400 nm and the emission peak appeared at 540 nm, which showed a 140 nm Stoke shift.[23] According to the authors, the phenomenon was due to the recombination of trapped charge carriers as opposed to free carriers. The trapping of the charge carriers occurs at surface defects that lie between the band gap states. In addition, the corresponding PL efficiencies were also measured and calculated by comparing to that for the 0.1 M quinine sulfate standard in sulfuric acid solution.[21] The

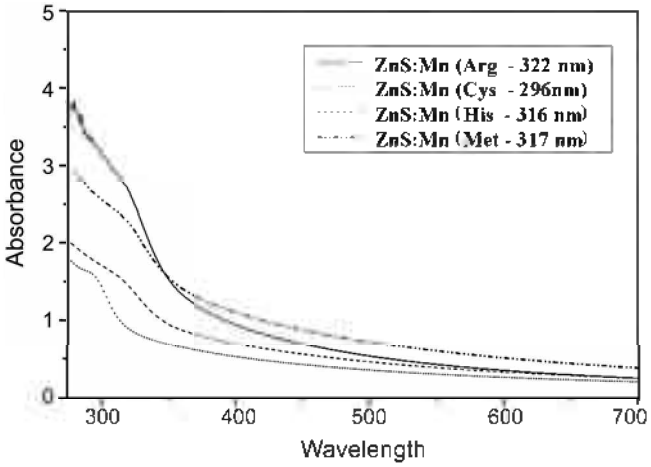

Figure 1. UV/Vis absorption spectra of aminoacids capped ZnS:Mn nanocrystals.

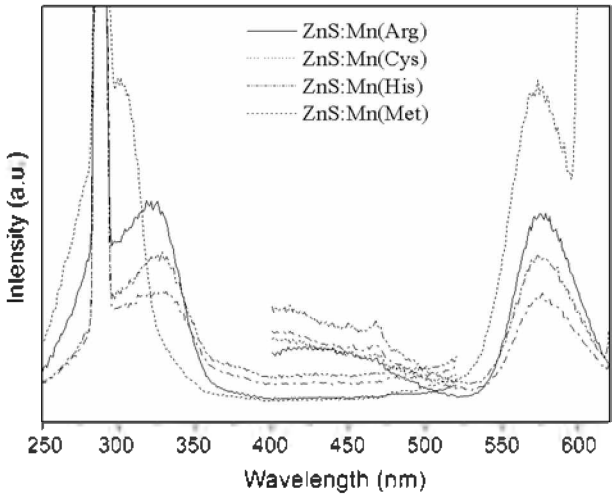

Figure 2. Room temperature solution photoluminescence excitation and emission spectra of aminoacids capped ZnS:Mn nanocrystals.

obtained PL efficiencies were 5.2% (Arg), 6.5% (Cys), 4.4% (His), and 7.1% (Met) respectively. The values are slightly lower than that for the previously mentioned valine capped ZnS:Mn nanocrystal (15.8%).

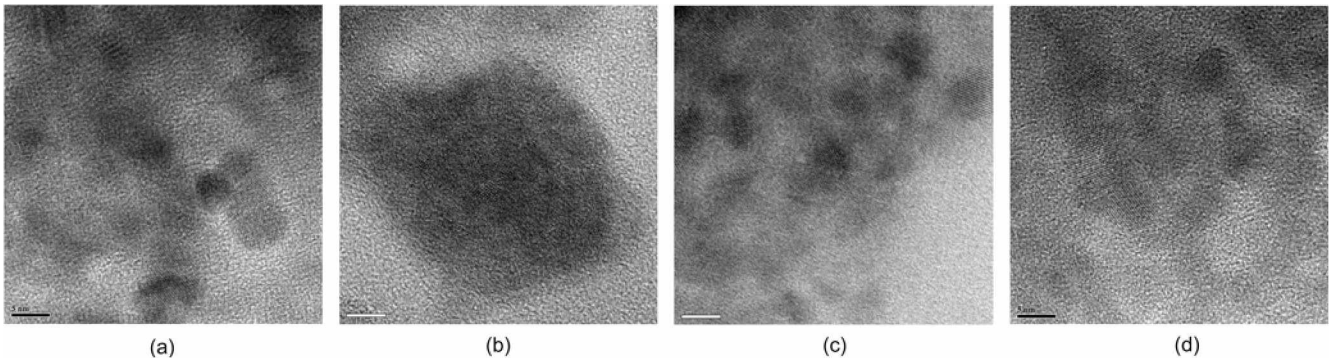

Figure 3. HR-TEM images of the aminoacids capped ZnS:Mn nanocrystals. The scale bar represents 5 nm. (a) HR-TEM image of ZnS:Mn (Arg) nanocrystal. (b) HR-TEM image of ZnS:Mn (Cys) nanocrystal. (c) HR-TEM image of ZnS:Mn (His) nanocrystal. (d) HR-TEM image of ZnS:Mn (Met) nanocrystal.

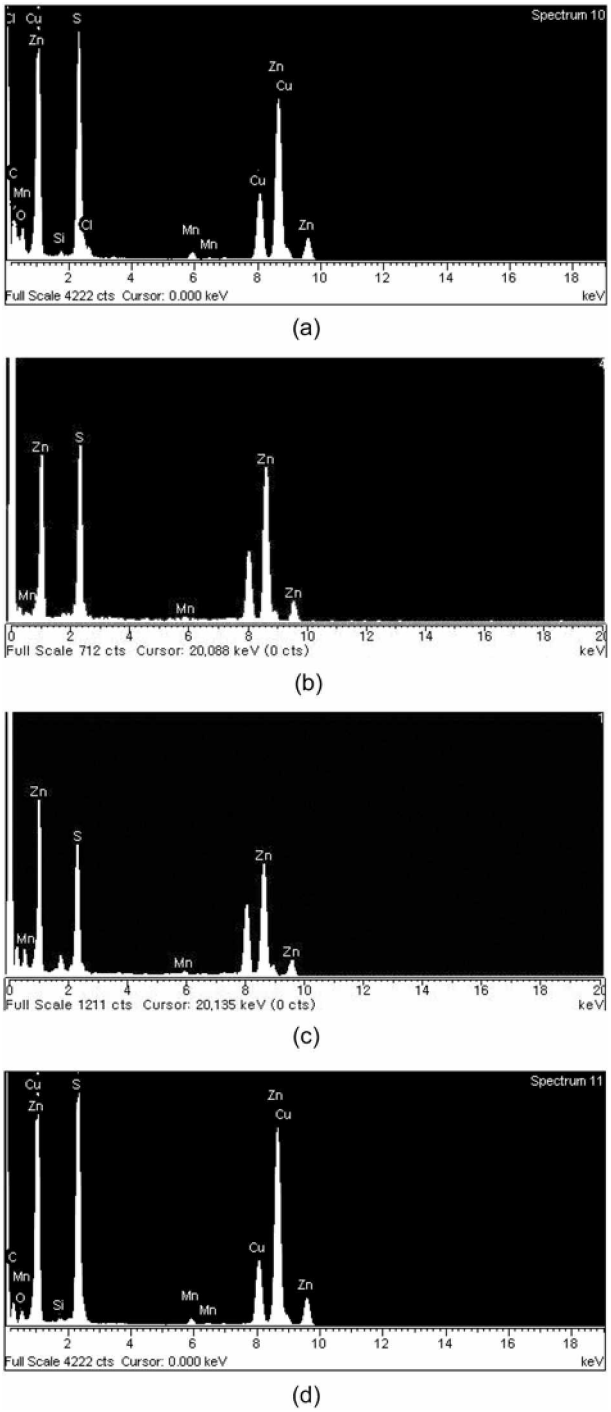

Figure 4. EDXS spectra for the aminoacids capped ZnS:Mn nanocrystals. (a) EDXS spectrum of ZnS:Mn (Arg) nanocrystal. (b) EDXS spectrum of ZnS:Mn (Cys) nanocrystal. (c) EDXS spectrum of ZnS:Mn (His) nanocrystal. (d) EDXS spectrum of ZnS:Mn (Met) nanocrystal.

The particle sizes of the corresponding aminoacids capped ZnS:Mn nanocrystals were measured *via* HR-TEM images presented in Figure 3. According to the images, the shapes of the particles are fairly homogeneous and the measured particle sizes are in the range of 5.3 to 11.7 nm, which are marginally bigger than that for the valine capped ZnS:Mn nanocrystal (3.3 nm in average). In the figures little

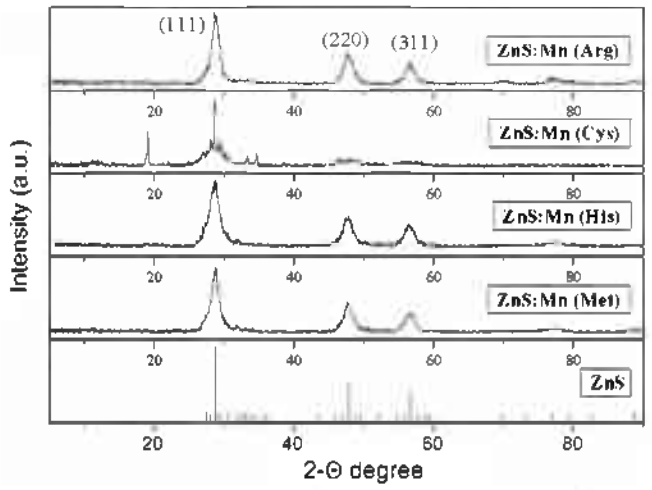

Figure 5. Powder X-ray diffraction pattern diagrams for the aminoacids capped ZnS:Mn nanocrystals.

agglomerations between the particles were observed due to the evaporation of the solvents during the sample preparation. However, the appearance of distinct lattice planes in the HR-TEM image with about 3 to 5 Å lattice spacing indicate that the obtained solids are made of single crystals rather than poly-crystalline aggregates for all the cases.

The EDXS diagrams were provided in Figure 4, which showed that the elemental compositions of the corresponding product solids. The diagrams confirm the formation of the ZnS:Mn nanocrystals in solid state. In addition, the EDXS elemental analysis also showed that the doping percentages of the manganese ions in the measured ZnS:Mn nanoparticles; 2.70% (Arg), 1.35% (Cys), 1.67% (His), and 2.31% (Met) respectively. It has been reported that the amount of the dopant usually affects the emission wave length for the bulk ZnS:Mn solid.[24] However, in our case, the effect of the amount of the dopant was not so significant since the emission wavelengths for the aminoacids capped ZnS:Mn nanocrystals were very similar to each other.

Figure 5 shows the wide angle X-ray diffraction patterns of powder samples of the aminoacids capped ZnS:Mn nanocrystals. In those diagrams, some of appeared peaks are too broad to be exactly assigned especially for the cysteine capped ZnS:Mn nanocrystal case. However, it is known as a quite common feature for most low-dimensional nano-sized materials. Even so, there were obviously indexable peaks such as (111), (220) and (311) planes in those diagrams indicating that the nanocrystals are in cubic zinc blende phases for all our amioacids capped ZnS:Mn nanocrystals.[25]

The corresponding aminoacid ligands on the surface of the ZnS:Mn nanocrystals were characterized by FT-IR spectroscopy as shown in Figure 6. The strong peaks appeared around 2950, and 1600 cm^{-1} were assigned as zinc coordinated $-NH_2$ and $-COO^-$ groups for corresponding aminoacids.[26,27] However, the peaks appeared around 2950 cm^{-1} were also possibly overlapped with that for C-H stretching bands in the aminoacid molecules.[28,29] To remove any uncoordinated or unreacted aminoacid molecules, the

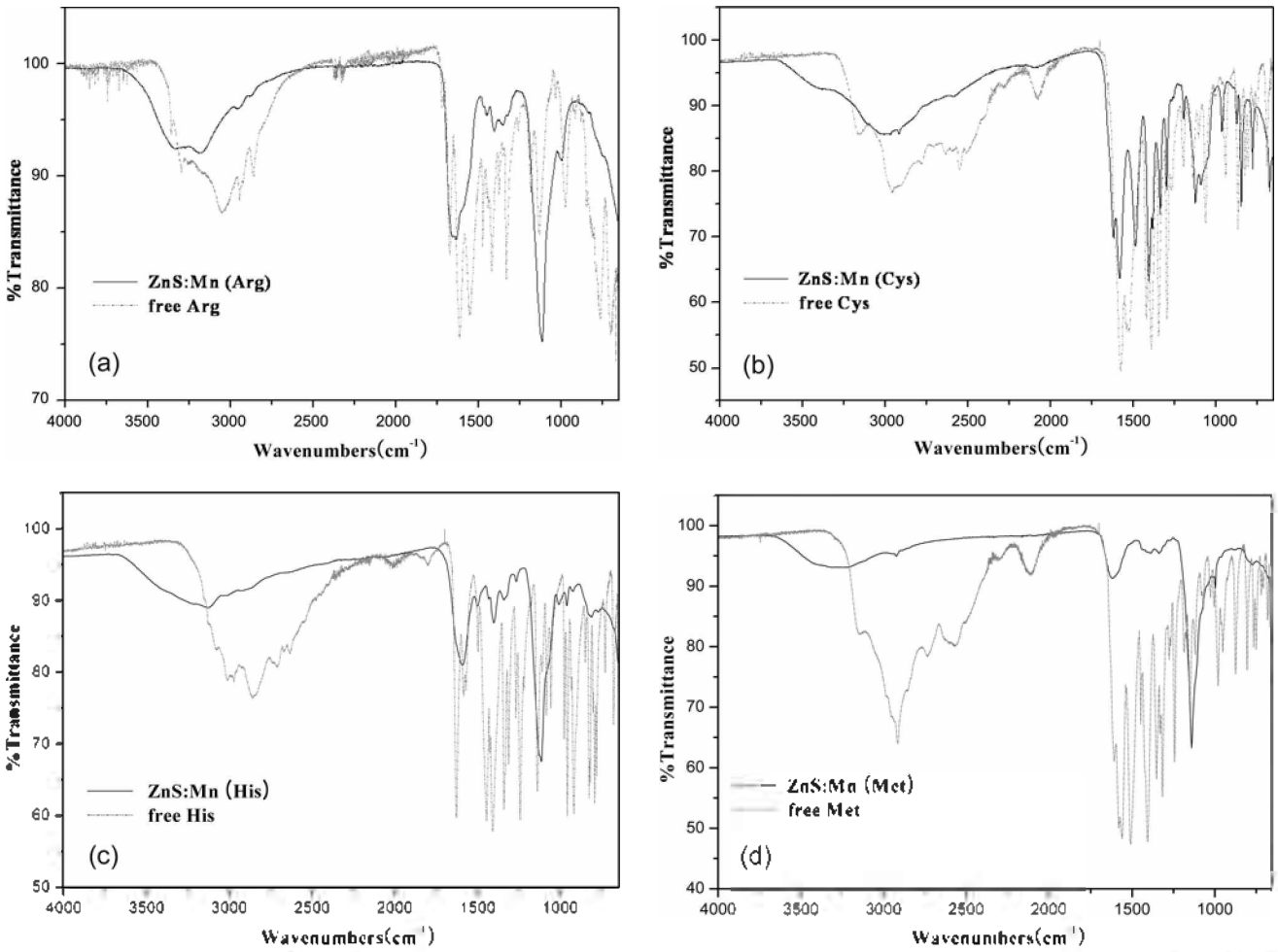

Figure 6. FT-IR spectra of the aminoacids capped ZnS:Mn nanocrystals. (a) FT-IR spectra of ZnS:Mn (Arg) nanocrystal (black line) with free arginine (red line). (b) FT-IR spectra of ZnS:Mn (Cys) nanocrystal (black line) with free cysteine (red line). (c) FT-IR spectra of ZnS:Mn (His) nanocrystal (black line) with free histidine (red line). (d) FT-IR spectra of ZnS:Mn (Met) nanocrystal (black line) with free methionine (red line).

centrifuged white solids were washed several times with cold alcohol/water mixture solutions rapidly. As a result, we were not able to find peaks resulted from the precursors, free aminoacid molecules, in the FT-IR spectra as demonstrated in the Figure 6. In addition, the spectra confirmed that all of the aminoacid ligands are attached on the surface of the ZnS:Mn nanocrystals to provide a water dispersible nature for the originally hydrophobic ZnS:Mn nanocrystals.

Conclusion

We have successfully synthesized water-dispersible ZnS:Mn nanocrystals by capping the originally hydrophobic surface of the nanocrystals with four kinds of aminoacids molecules: arginine, cystein, histidine, and methionine. Those obtained colloidal nanocrystals were measured for their optical properties by UV/Vis, room temperature solution PL spectroscopies, and further obtained powders were characterized by XRD, HR-TEM, EDXS, and FT-IR spectroscopy analyses. The solution PL spectra showed broad emission peaks around 580 nm and with PL efficiencies in the range of 4.4 to 7.1%. In addition, the measured particle sizes for the aminoacid capped ZnS:Mn nanocrystals *via* HR-TEM images were in the range of 5.3 to 11.7 nm. One of the reasons that we synthesized the water-soluble ZnS:Mn semiconductor nanocrystal is to bind it to biomolecules, such as DNA and protein, so that they can be used as a biosensor material. In that point of view, the water soluble aminoacids capped ZnS:Mn nanocrystals showed sufficient physical and chemical properties to be applied to a microchip-scale biosensor system.

Acknowledgement. This work was supported by Seoul R&BD Program (10555cooperateOrg92862).

References

1. Weller, H. *Angew. Chem. Int. Ed. Engl.* **1993**, *32*, 41.
2. Bol, A. A.; Meuijernk, A. *Phys. Rev. B* **1998**, *24*, 58.
3. Alivisatos, A. P. *J. Phys. Chem.* **1996**, *100*, 13226.
4. Brus, L. E. *Appl. Phys. A: Solid Surf.* **1991**, *53*, 465.
5. Milliron, D. J.; Alivisatos, A. P.; Pitois, C.; Edder, C.; Frechet, J. M. *J. Adv. Mater.* **2003**, *15*, 58.
6. Jaiswal, J. K.; Mattoussi, H.; Mauro, J. M.; Simon, S. M. *Nature Biotechnol.* **2002**, *21*, 47.

7. Heath, J. R. *Acc. Chem. Res.* **1999**, 32.
8. Hoffman, A. J.; Mills, G.; Yee, H.; Hoffmann, M. R. *J. Chem. Phys.* **1992**, *96*, 5546.
9. Kanemoto, M.; Shiragami, T.; Pac, C.; Yanagida, S. *J. Phys. Chem.* **1992**, *96*, 3521.
10. Dabbousi, B. O.; Bawendi, M. G.; Onitsuka, B. O.; Rubner, M. F. *Appl. Phys. Lett.* **1995**, *66*, 11.
11. Hwang, J. M.; Oh, M. O.; Kim, I.; Lee, J. K.; Ha, C.-S. *Curr. Appl. Phys.* **2005**, *5*, 31.
12. Yu, S. H.; Wu, Y. S.; Yang, J. *Chem. Mater.* **1998**, *9*, 2312.
13. (a) Gerion, D.; Pinaud, F.; Williams, S. C.; Parak, W. J.; Zanchet, D.; Weiss, S.; Alivisatos, A. P. *J. Phys. Chem. B* **2001**, *195*, 8861. (b) Jun, Y. W.; Jang, J. T.; Cheon, J. W. *Bull. Kor. Chem. Soc.* **2006**, *27*, 961.
14. Chen, C. C.; Yet, C. P.; Wang, H. N.; Chao, C. Y. *Langmuir* **1999**, *15*, 6845.
15. Mitchell, G. P.; Mirkin, C. A.; Letsinger, R. L. *J. Am. Chem. Soc.* **1999**, *121*, 8122.
16. Kho, R.; Nguyen, L.; Torres-Martinez, C. L.; Mehra, R. K. *Biochem. Biophys. Res. Commun.* **2000**, *272*, 29.
17. Bae, W.; Mehra, R. K. *J. Inorg. Biochem.* **1998**, *70*, 125.
18. Bhargava, R. N.; Gallagher, D. *Phys. Rev. Lett.* **1994**, *72*, 416.
19. Yi, G.; Sun, B.; Yang, F.; Chen, D. *J. Mater. Chem.* **2001**, *11*, 2928.
20. Hwang, C. S.; Lee, N. R.; Kim, Y. A.; Park, Y. B. *Bull. Kor. Chem. Soc.* **2006**, *27*, 1809.
21. Williams, A. T. R.; Winfield, S. A.; Miller, J. N. *Analyst* **1983**, *108*, 1067.
22. Melhuish, W. H. *J. Phys. Chem.* **1961**, *65*, 229.
23. Tata, M.; Banerjee, S.; John, V. T.; Waguespack, Y.; Mcpherson, G. *Coll. Surf. A Phys. Chem. and Eng. Asp.* **1997**, *127*, 39.
24. Kushida, T.; Tanak, Y.; Oka, Y. *Sol. Stat. Commun.* **1974**, *14*, 617.
25. Zhuang, J.; Zhang, X.; Wang, G.; Li, D.; Yang, W.; Li, T. *J. Mater. Chem.* **2003**, *13*, 1853.
26. Moszczenski, C. W.; Hooper, R. J. *Inorg. Chim. Acta* **1983**, *70*, 71.
27. Nakamoto, K. *Infrared and Raman Spectra of Inorganic and Coordination Compounds*. Part B. 5th Ed.; Wiley: 1997; p 59.
28. Pandiarajan, S.; Umadevi, M.; Rajaran, R. K.; Ramakrishinan, V. *J. Spectrochim. Acta A* **2005**, *62*, 630.
29. Pawlukojic, A.; Leciejewicz, J.; Ramirez-Cuesta, A. J.; Nowicka-Sciebe, J. *Spectrochim. Acta A* **2005**, *61*, 2474.